Self-resistance electric heating of shaped CFRP laminates: temperature distribution optimization and validation

Yingxiang Shen
Yong Lu (luyong@njit.edu.cn)
Nanjing Institute of Technology
Shuting Liu
Qiangqiang Liu
Shuangquan Tao
Xiaozhong Hao

Research Article

Keywords: Reinforced polymer, Self-resistance electric heating, Multi-zone heating, Uniform temperature, Curing

Posted Date: February 28th, 2022

DOI: https://doi.org/10.21203/rs.3.rs-1205750/v1

Self-resistance electric heating of shaped CFRP laminates: temperature distribution optimization and validation

Yingxiang Shen[1], *Yong Lu[2]， Shuting Liu[1]， Qiangqiang Liu[1]， Shuangquan Tao[1], Xiaozhong Hao[1]

1. College of Mechanical and Electrical Engineering, Nanjing University of Aeronautics and Astronautics, Nanjing, 210016, China.

2. School of Mechanical Engineering, Nanjing Institute of Technology, Nanjing, 211167, China.

Abstract: The Self-Resistance Electrical (SRE) heating method to cure carbon fiber reinforced polymer (CFRP) part possesses the advantages of rapid and volumetric heating, low energy consumption, and low asset investment. But the current SRE heating methods are difficult to uniformly cure the shaped CFRP parts due to the non-uniformly distributed Joule heat power in the parts with a varying cross-sectional area. In this paper, an optimized multi-zone SRE heating method is proposed, in which the uniform heating and curing process of the shaped CFRP part is firstly achieved. By optimizing the orientation of the rectangular zones, the local overheating caused by the voltage gradient and current diffusion between different zones is notably suppressed. Combined with the electro-thermal numerical analysis, the influence of the positional offset of electrodes in two adjacent zones on the temperature uniformity is investigated. Based on this, an automated zoning algorithm and the prioritizing method of the zone orientation are established. The proposed method is numerically and experimentally validated with the typical shaped CFRP parts, and the results are compared with that of the existing SRE heating method. The proposed method realizes that the maximum in-plane temperature difference of shaped CFRP parts is reduced by more than 80%. This method significantly improves the temperature uniformity of shaped CFRP parts during the multi-zone SRE heating process, which provides a potential solution for high-quality and efficient curing of CFRP parts.

Key words: Reinforced polymer, Self-resistance electric heating, Multi-zone heating, Uniform temperature, Curing

1.Introduction

Due to superior mechanical properties such as lightweight and high strength, carbon fiber reinforced plastics (CFRP) have gained huge applications in many fields including aerospace, automotive, and maritime [1-6]. The curing process where the CFRP part acquires the geometrical shape and mechanical properties simultaneously, is the key step to ensure the quality of CFRP products. Currently, the autoclave curing process is the dominant technology for curing high-performance CFRP parts [7,8]. However, owing to the thermal conductive-based heating mechanism, the autoclave curing process presents the disadvantage of thermal lagging, long cycle time, high energy consumption, and high equipment investment [9]. In recent years, Out-of-Autoclave (OoA) curing technologies have attracted wide attention [10-13]. Among these technologies, the self-resistance electrical (SRE) heating method that directly utilizes the electric current passing through the carbon fiber itself to produce a massive Joule heat, can realize a promising curing process with a number of advantages such as volumetric heating, rapid heating, low energy consumption, and low asset investment [14].

However, at present, the SRE heating method can only uniformly heat the CFRP part with a constant cross-sectional area along the electrical current path, for example, the rectangular blank part. Due to the existence of the

* Corresponding author: Yong Lu, Email: luyong@njit.edu.cn
Yingxiang Shen, Email: yxshen@nuaa.edu.cn
Shuting Liu, Email: liushooting@nuaa.edu.cn
Qiangqiang Liu, Email: liuqq@nuaa.edu.cn
Shuangquan Tao, Email: nuaa_tsq@nuaa.edu.cn
Xiaozhong Hao, Email: xhao@nuaa.edu.cn

varying cross-sectional area, the non-uniformly distributed current density and the Joule heat power are inevitably formed in the non-rectangular or shaped CFRP part. In practical aerospace and other industries, most CFRP parts such as wing-skin and hatch parts are non-rectangular and possess shaped geometries. Therefore, the uniform SRE heating of shaped CFRP parts is a major challenge needing to be solved urgently.

To solve the above challenge, the existing methods can be divided into the following two categories. Both of these reported methods focused on the SRE heating of metal parts, but they could also provide a research basis for the SRE heating of CFRP parts. The first category is the integral compensation (IC) method, where the extra material is added to the edge of the shaped part to form an integral rectangular so that the current density, as well as the Joule heat power of the part, can be uniformly distributed. In the patent published by Benteler Corporation [15], a shaped blank was compensated by using the same material to make a structure with a constant cross-section area, and uniform SRE heating of the compensated structure was achieved, and then the final part was obtained after the compensated material being cut off. In the patent published by Toyota Corporation [16], a rectangular compensation method for shaped parts with holes was proposed, in which the metal material was used to fill the holes inside the part to extend an additional current path and the uniform current density could be realized. The above methods achieved the uniform SRE heating of shaped metal parts, but they were difficult to avoid introducing a massive redundant material and thus resulted in unnecessary energy consumption. In addition, the practical shaped CFRP parts are usually cured on tools of limited size, and the IC methods are difficult to be achieved under the limited tool boundary size in the curing process of CFRP parts.

The second category is the multi-zone compensation (MZC) method, where the shaped part is divided into several rectangular strips by introducing multiple pairs of electrodes and the power of each strip is independently controlled by a specific generator [17-19]. Hübner et al. [20] developed an MZC method where the metal sheet was compensated with similar material and several paralleled rectangles were formed. By utilizing multiple independent power generators, the heating power could be independently controlled according to the length of each rectangle. To minimize the compensational material usage, Demazel et al. [21] proposed a solution where the part was split into several rectangular strips heated by multiple generators, and they optimized the orientation and dimensions of rectangular strips to reduce the material and energy usage. The above MZC methods achieved uniform SRE heating of shaped parts with lower energy consumption and material usage compared to the IC methods. However, although the current MZC methods can achieve an acceptable temperature field within the net-shape area, there is still a large temperature gradient within the entire conductive structure, especially at the adjacent area between different rectangular strips. This can be attributed to that the existing methods do not consider the transverse voltage gradient and the transversely diffused current between different zones, which are caused by the positional offset of the electrodes in adjacent zones and result in local overheating and the large in-plane temperature gradient (in-plane temperature difference greater than 60 °C). But the maximum temperature difference that most CFRP materials would not present thermal degradation is below 20 °C when the average temperature reaches 120 °C. [22]. Hence, it is necessary to improve the MZC methods considering the transverse current diffusion between adjacent strips to achieve uniform SRE heating of shaped CFRP parts.

In this paper, an optimized multi-zone SRE heating method considering the minimized positional offset of equipotential points in adjacent strips is proposed, in which the transverse voltage gradient and the local overheating caused by current diffusion are notably suppressed by optimizing the orientation of strips. The uniform heating and curing process of the shaped CFRP part is firstly achieved by using the proposed method. Combined with the COMSOL multiphysics® electro-thermal model, the influence of the VCC (voltage common connector) and GND (ground) electrodes positional offset on the temperature uniformity is investigated. Based on this, an automated zoning algorithm and the optimal selection method of the strip orientation are established. The SRE heating temperature field and current diffusion results of the typical shaped CFRP parts under the proposed and the traditional

methods are compared. In addition, for a practical shaped CFRP wing-skin part, the multi-zone SRE heating processes are implemented using the multi-power system, and the effectiveness in improving the temperature uniformity of the presented method is evaluated and compared. This method significantly improves the temperature uniformity of shaped CFRP parts during the SRE heating process, which provides a potential solution for the high-quality and efficient curing of CFRP parts.

2. Influential analysis of the VCC and GND electrodes positional offset in adjacent strips on the temperature field

The current MZC methods can potentially realize the uniform SRE heating for the shaped CFRP parts. However, the existing methods do not consider the transverse voltage gradient caused by the positional offset of the electrodes in adjacent strips, which results in local overheating. The electric potential inside each strip is actually related to the applied voltage across the ends of the strip, and can be influenced by the position of the GND and VCC electrodes relative to the counterparts of adjacent strips. Therefore, to find an optimal solution that can minimize the in-plane temperature difference, this section analyzes the influence of the GND and VCC electrodes positional offset in adjacent strips on the SRE heating temperature field via the electro-thermal FEM (finite element modeling) method.

2.1 Electro-thermal finite element modeling

The 3D electro-thermal FEM using COMSOL Multiphysics® software is developed to simulate the SRE heating process. In the multi-zone SRE heating method, the shaped part is discretized into multiple rectangular strips. In order to simplify the analysis process, a local structure with two adjacent strips is selected in the 3D model, where the positions of the GND and VCC electrodes of each strip are set as the variable parameters. This model is based on the Joule's law and solid heat transferring theory [23-25]. The thermal and electrical parameters of the cross-plied CFRP laminate are given in Tab.1.

3D geometry model: As shown in Fig.1, each strip has the same thickness and width, and the variable positional offset of the GND (0 V) electrodes of two strips is defined as l, and the lengths of the strips are L_1 and L_2 respectively. Define the relative offset of two GND electrodes as: $l/L2$. The maximum length of L_1 and L_2 is set to 400 mm, and the corresponding maximum VCC voltage is given by 1 V.

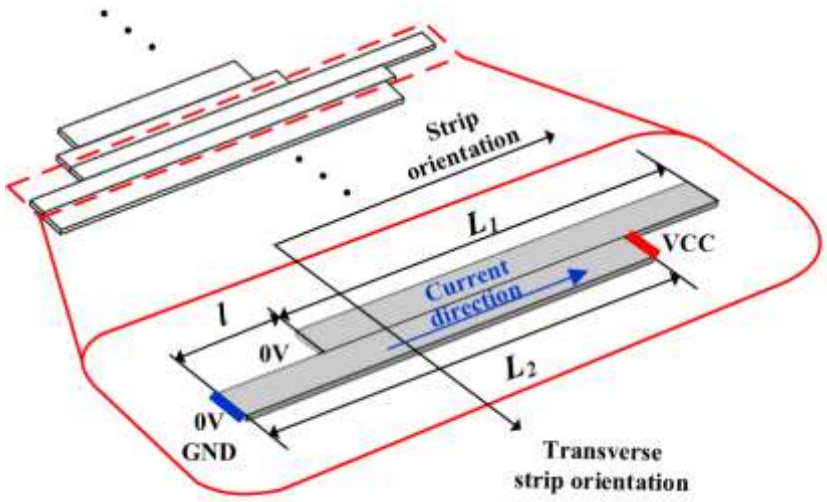

Fig.1 Schematic of the 3D structure used for investigating the effect of temperature field uniformity

Concepts definition: The strip orientation is defined as the direction along the connection line between the VCC and GND electrodes in a specific rectangular strip. Under ideal conditions, there is no voltage gradient in the transverse orientation between the adjacent two strips, and the current is expected to flow along the strip orientation.

Electro-thermal coupled FEM: The electric Joule heating model of CFRP laminate is established to simulate

the Joule heating process of CFRP laminate during the SRE heating process. The thermal balance equation is given by the following equation[26]:

$$\rho \cdot Cp \cdot \frac{\partial T}{\partial t} = \nabla(\overline{\overline{k}} \nabla T) + \vec{E} \cdot \vec{J} - \dot{Q}_{losses} \tag{1}$$

where ρ and Cp are the density and specific heat capacity of the CFRP material, respectively. $\overline{\overline{k}}$ is the thermal conductivity tensor. The generated heat per unit time and volume is the dot product of the electric field and the current density ($\vec{E} \cdot \vec{J}$). $\dot{Q}_{losses}$ is the external heat dissipation per unit volume of composite material. The current density is expressed by the simplified form:

$$\vec{J} = \overline{\overline{\sigma}} \vec{E} \tag{2}$$

where $\overline{\overline{\sigma}}$ is the electrical conductivity tensor.

The relevant material parameters are shown in the following Tab.1, and the data were obtained from actual measurements of CFRP composite parameters by previous work [27].

Tab.1 Mechanical, thermal and electrical properties of CFRP laminates

parameter	properties	value	unit
ρ	density	1578	kg/m^3
C	Specific heat	1260	J/(kg·K)
σ	Electrical conductivity	{6×10^5,6×10^5,4.67}	S/m
ε	Relative dielectric constant	3.856	1
k	Thermal conductivity	{2.33,2.33,0.56}	W/(m·K)

Voltage control method in the FEM： To ensure that the temperature in each strip is equal, it is necessary to apply a specific value of VCC voltage according to the material and dimensions of each strip. In the FEM, the VCC voltage of each strip is proportionally controlled according to the monitored deviation of the temperature feedback from the target temperature. Assuming that the temperature distribution of each strip is uniform and the temperature value is only affected by the VCC voltage of that area, the heating rate r of that strip can be derived by the simplified equation:

$$r = \frac{\sigma \cdot U^2}{Cp \cdot \rho \cdot L^2} \tag{3}$$

where σ is the electrical conductivity along the lengthwise direction [S/m], U is the VCC voltage [V], L is the length of that rectangular strip [m]. From the equation, the heating rate r of a single strip is only related to the length L and the VCC voltage of that strip, and is independent to the thickness and width. Therefore, the VCC voltage is approximately proportional to the length L of each strip if the heating rate r of each strip is required to be equal.

The above section introduces the FEM method of the multi-zone SRE heating process in a local structure with two adjacent strips. The following sections give the detailed analysis of the temperature field distribution and its formation mechanism under different positional offset parameters of the GND and VCC electrodes.

2.2 The influence of the GND electrodes positional offset on the temperature field

Each strip has a GND electrode or the negative equipotential end. If the positions of the GND electrodes of adjacent strips are shifted, the transverse voltage gradient and the accompanying currents must form between the strips, leading to local overheating. Combined with the above FEM model, this section discusses the influence of the GND electrodes positional offset in two adjacent strips on temperature field.

As shown in Fig.2a, when there is no positional offset two GND electrodes, the parallel and equidistant equipotential lines are formed inside the strips. Therefore, it can be seen from Fig.2b that the current does not diffuse transversely but is evenly distributed in the strip, which makes the final temperature field uniformly distributed.

However, due to the complex contour of the shaped part, the final position of the adjacent strips could possibly be arranged as shown in the lower graph of Fig.2a. In this case, the GND end of the upper strip is located in the middle of the lower strip, which directly leads to a transverse voltage difference of about 0.1 V. Hence, it can be seen that the equipotential lines are bent there, and the current lines in Fig.2b are not distributed at equal intervals but are locally concentrated, which means the higher current density is presented in these concentration points. Naturally, due to the increased current density, local overheating occurs, while the other side of the strip is not effectively heated as shown in Fig.2c, and the maximum in-plane temperature difference reaches 100 °C. To sum up, if the existing MZC method does not consider the GND positional offset of each strip, local overheating and the non-uniform temperature field can be inevitably formed in the multi-zone SRE heating of CFRP parts.

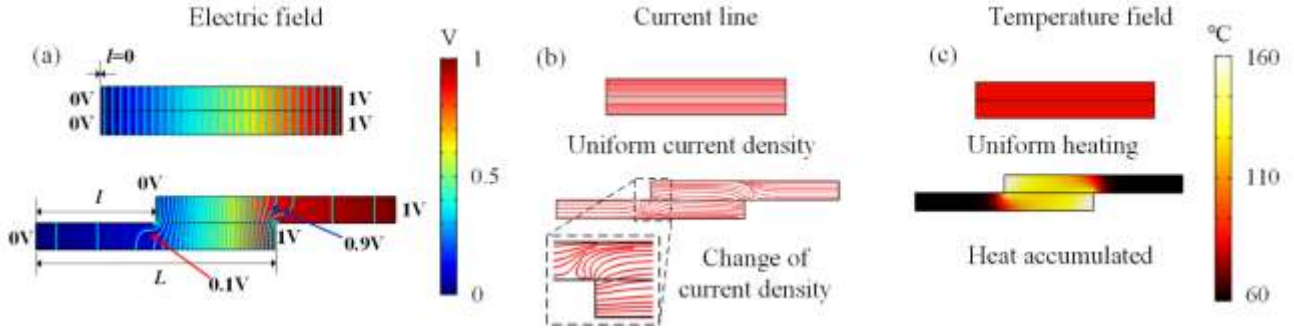

Fig.2 Schematic of positional offset of GND electrodes influence. **a** influence on the electric potential field, **b** influence on the current line, **c** influence on the temperature field

Further, in order to quantitatively analyze the influence of the positional offset of the GND electrodes on the temperature field, change the value of the relative offset of GND from 0-100%, and the change of the maximum in-plane temperature difference is shown in Fig.3. Set the length of *L1* and *L2* equal to 400 mm, and apply the same VCC voltage of 1 V to both strips. The value of each dot in Fig.3 is measured when the average in-plane temperature reaches 120°C. As can be seen in Fig.3, the greater relative offset of the GND electrodes, the greater in-plane temperature difference in both strips. When the relative offset exceeds 90%, the in-plane maximum temperature difference has reached more than 300°C. The upper limit offset value that can result in an acceptable in-plane temperature difference (≤20°C) is 8.2% in this case.

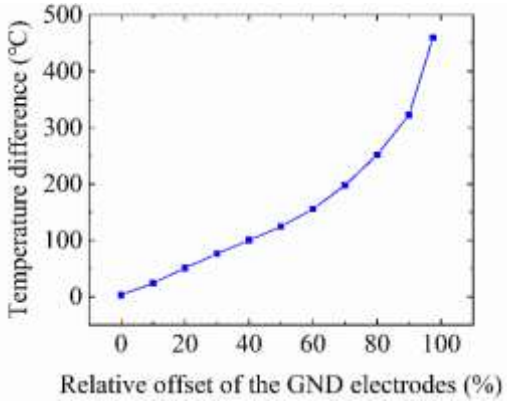

Fig.3 Temperature difference as a function of relative position of the GND electrodes

This section focuses on the influence of the GND electrodes offset on the temperature field. A larger GND positional offset results in a larger in-plane temperature difference. Therefore, for an arbitrary shaped CFRP part, the orientation of the multiple strips should be appropriately selected to ensure the minimum offset of the GND electrode of final strips structure. The following describes the influence of the positional offset of the VCC electrodes on the temperature field.

2.3 The influence of the VCC electrodes positional offset on the temperature field

According to the Eq.3, the VCC voltage is proportional to the length L of each strip if the heating rate r of each strip is required to be equal. Therefore, if there is no positional offset of GND electrodes, as shown in Fig.4a, the voltage values applied to the VCC electrodes that are offset to each other should be related to the lengths of corresponding strips. As can be seen in Fig.4a, in this case, although there is a positional offset between the two VCC electrodes, there is no transverse voltage gradient, and the equipotential lines are still parallel and equidistant. Hence, there is no local concentration of the current lines, and the final temperature field remains uniform, as shown in Fig.4b and c.

However, in the actual voltage control process, due to the fluctuation of the input voltage and heat dissipation, the VCC voltage of each strip cannot always maintain in a stable condition, which directly results in the transverse voltage gradient and the accompanying local overheating. Therefore, it is necessary to adjust the parameters of the generators to ensure that the input voltage can be stable as much as possible, and thermal insulation for the entire part is also required to minimize the thermal dispassion difference of multiple strips.

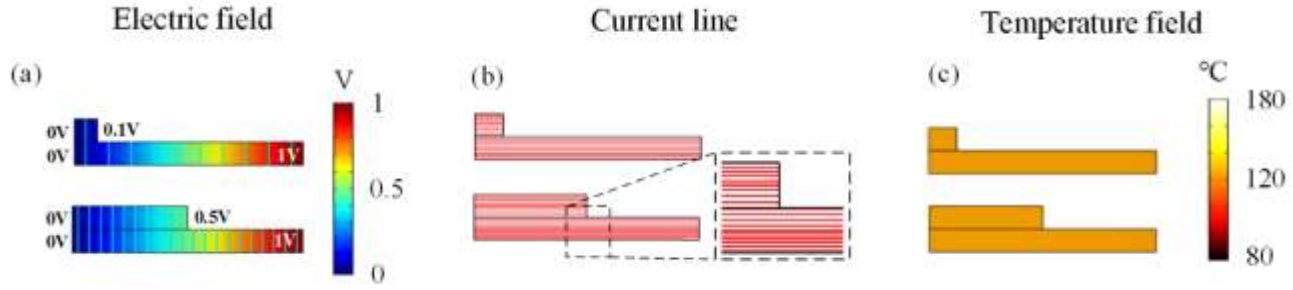

Fig.4 Schematic of positional offset of VCC electrodes influence. **a** influence on the electric potential field, **b** influence on the current line, **c** influence on the temperature field

From the above analysis, the positional offset of the GND electrodes has a significant impact on the final temperature uniformity, which should be avoided as much as possible. On the other hand, the offset of VCC electrodes has less influence on the temperature field, but it is necessary to ensure the input VCC voltage values to be maintained in a stable condition. For shaped CFRP parts, the positional offset of GND electrodes can be effectively minimized by regulating the orientation of strips. The optimized multi-zoning methodology for shaped CFRP parts considering the minimized positional offset of equipotential points in adjacent strips is introduced below.

3. Multi-zoning methodology for shaped CFRP parts

Based on the analysis in Chapter 2, the temperature uniformity can be effectively improved by adjusting the strip orientation of shaped CFRP parts. Therefore, the fundamental to improving temperature uniformity is to find an orientation that minimizes the transverse voltage gradient and the accompanying local overheating. This chapter mainly develops an optimized multi-zoning method to achieve the uniform temperature field during the SRE heating process.

The main idea of the presented method is to quickly obtain the strips discretization results in all orientations (0-180°) and then prioritize the optimal orientation that has the smallest GND electrodes offset. Specifically, in this chapter, an automatic strips discretization (ASD) algorithm is firstly established, and then the principle of optimal orientation prioritizing is given. Finally, the effectiveness of this method is validated and compared with the traditional method via process simulation of two typical CFRP parts.

3.1 Automated strips discretization algorithm

In this section, the ASD algorithm considering the boundary constraints is established. The overall idea of the ASD algorithm is to discretize the CFRP part into a minimum number of strips under the boundary constraints along

with a certain orientation, and then to quickly iterate this discretization operation from all orientations between 0-180°.

As shown in Fig.5, for an arbitrary CFRP part, there are two boundaries to be considered in the ASD algorithm. The inner boundary is the net-shape boundary (the contour line of the unfolded surface for the 3D part) of the CFRP part, which is also the cutting path after the cure. The outer boundary is the contour of the CFRP preform during the fiber placement, which ensures that there is enough space to place auxiliary materials such as vacuum sealing tape at the edge of the tool [28]. For the discretization operation of a certain orientation, the ASD algorithm is based on the computation principle that the position and size of each strip are determined by the intersections of the lines and the two boundaries. This principle can ensure maximum usage of the material inside two boundaries and a minimized number of strips in each orientation.

For example, as shown in Fig.5, firstly, a horizontal line is drawn from the lowermost vertex of the inner boundary to get the tangent and intersection with the inner and outer edges, respectively. Secondly, the intersection of the horizontal line is selected with the left outer border and the right vertex of the inner border to draw vertical lines 1 and 1' up. Thirdly, compare the lengths of 1 and 1', and select the vertical line 1 that does not exceed the outer boundary after forming the rectangle as the side of the first rectangular area. Fourthly, a horizontal line passes through the intersection of vertical line 1 and the inner boundary, which is the upper boundary of the first rectangular area. Then the left and right ends of the first upper boundary are extended again, intersecting the inner and outer boundaries respectively. The intersection of the strip boundary control is selected again, and a vertical line is drawn from the selected intersection, extending upwards. Then compare the lengths of 2 and 2', and take the vertical line 2 that does not exceed the outbound boundary after forming the rectangle as the side of the second rectangular area. Each orientation of strip discretization takes about 1 second to calculate, and the calculation process of all orientations between 0-180° takes about 1 minute.

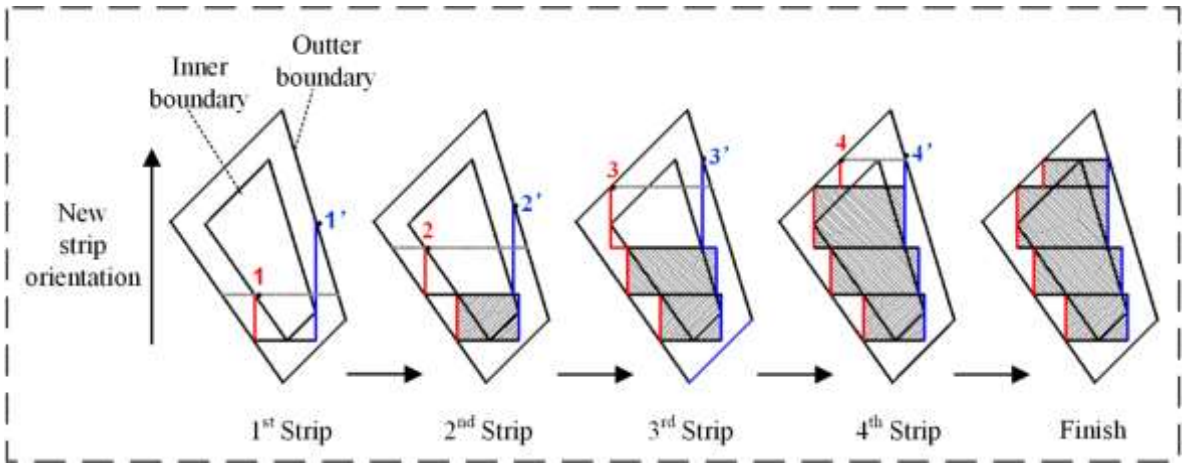

Fig.5 Schematic of ASD algorithm

This section establishes the ASD algorithm, which can rapidly realize the strip discretization of a shaped CFRP part along with all orientations between 0-180° in seconds. The ASD algorithm provides a basis for the prioritizing operation of orientation to improve the temperature uniformity during the SRE heating process.

3.2 Prioritizing principle of strips orientation

According to the conclusion of Chapter 2, the smaller positional offset of the GND electrodes of adjacent strips can lead to a more uniform temperature field, and the offset of VCC electrodes is independent to the temperature field. Therefore, the principle to select the optimal orientation is to find an orientation in which the positional offset of the GND electrodes is the smallest one among that of all orientations. Considering the discretization result along each orientation obtained from the ASD algorithm has two different sides (waiting for assignment of VCC and GND end), before calculating the positional offset of the GND electrodes, it is necessary to determine the side of applied

the GND electrode. The specific steps to find the optimal strip orientation are as follows, as shown in Fig.6.

1. Starting from the initial strip orientation (0°), calculate the position offsets of all adjacent rectangular strips, as shown in Fig.6. In this case, initial orientation has four strips and has three positional offsets on each side. Offsets at both sides of strips are named as l_a, l_b, l_c, and l_1, l_2, l_3, separately.

2. Record the maximum offset of both sides of the adjacent strip, and take the side with the smaller offset as the GND electrodes. In the case of the initial orientation, l_b and l_3 are the maximum offsets, and l_b is the smaller one. So take the side (blue) with a smaller positional offset as the GND electrodes side.

3. The optimal strip orientation has the smallest offset of the GND electrodes position among all strip orientations. After that the maximum positional offset of the GND electrodes of all orientations between 0-180° are obtained, select the strips orientation with minimum positional offset as the best strips discretization orientation. In this case, the optimal orientation is θc, where the minimum positional offset of GND electrodes is 0 mm.

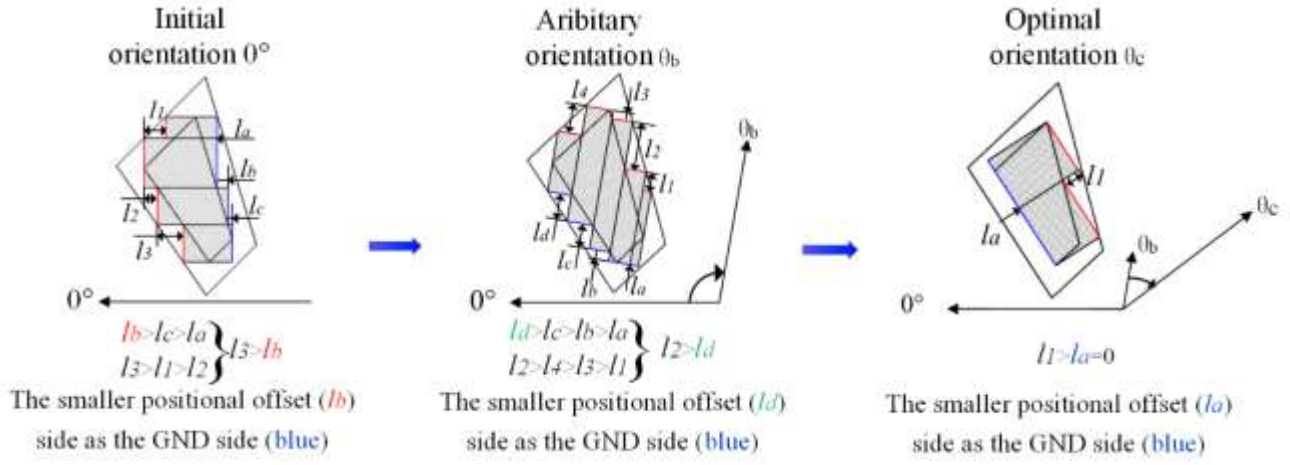

Fig.6 Schematic of prioritizing the optimal orientation according to the minimum positional offset of GND electrodes

From the above method, an optimal orientation that minimizes the positional offset of GND electrodes can be rapidly prioritized for an arbitrary shaped CFRP part. This orientation is expected to be the optimized multi-zoning solution to improve the temperature uniformity. Next, the effectiveness of this method is discussed and analyzed with the simulation results of two typical CFRP parts.

3.3 FEM validation and comparative analysis

Two typical shaped CFRP parts are selected to test the presented method. These parts both present irregular shape and cannot be uniformly heated by the traditional SRE heating method, as shown in Fig.7. By running the ASD algorithm, the results of the maximum positional offset of the GND electrodes along with every orientation (0-180°, step length 2.8125°, 64 steps) can be computed. According to the prioritizing principle described above, the optimal orientation can be found among the results. Then, the SRE heating temperature fields of the shaped parts are simulated by the COMSOL software both under the initial and the optimized orientations. The specific analysis is as follows.

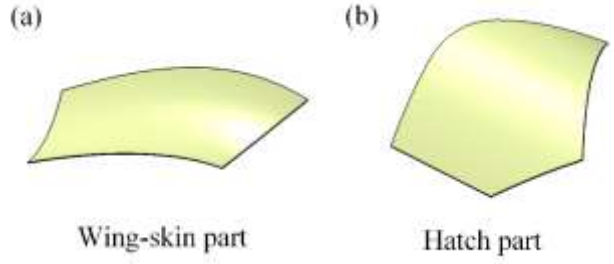

Fig. 7 Two typical CFRP part **a** Wing-skin part **b** Hatch part

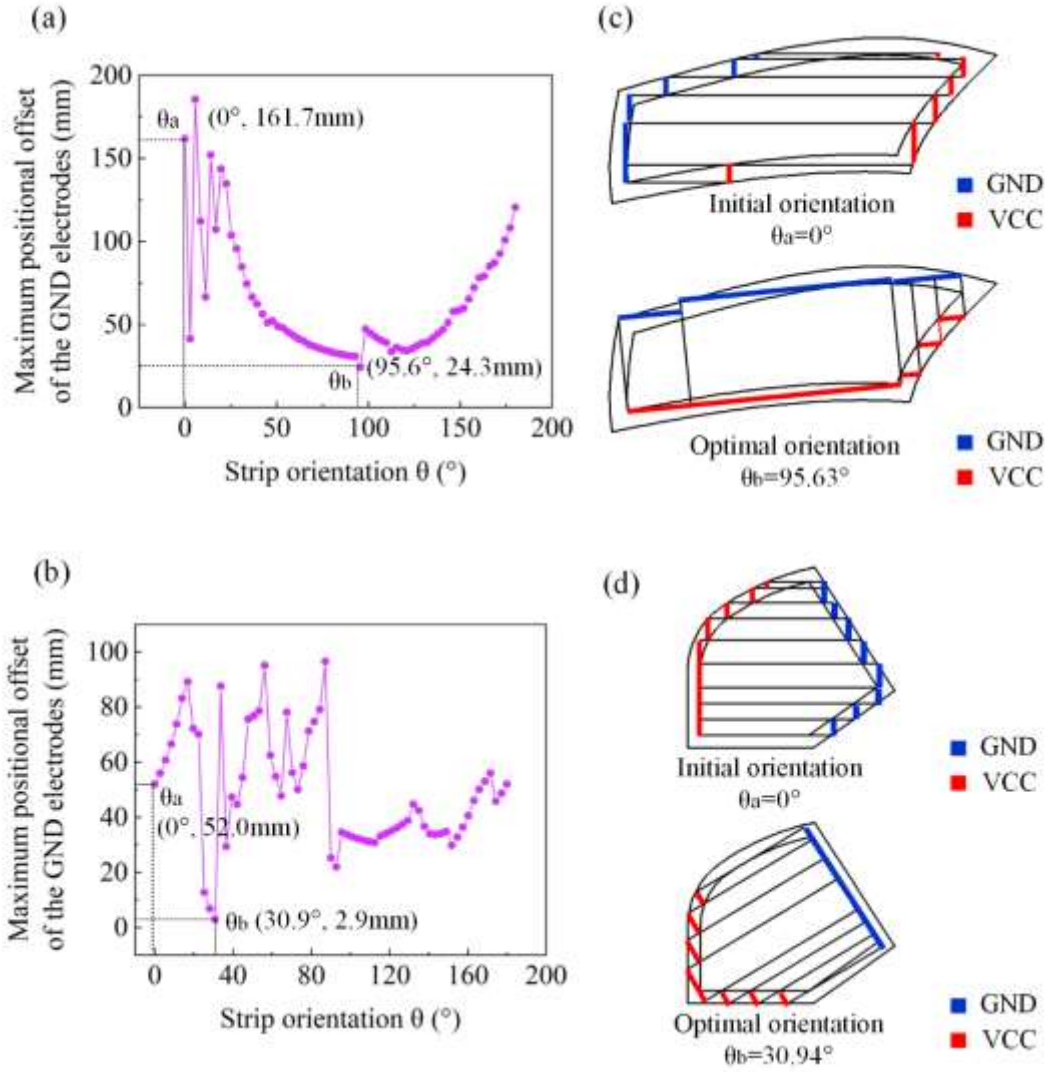

Fig.8 Prioritizing results of two typical parts **a,b** maximum positional offset of the GND electrodes for the wing-skin and the hatch part, **c,d** the rectangular strip arrangements of the initial and optimal orientation for the wing-skin and the hatch part

The results of the maximum positional offset of the GND electrodes for the wing-skin and the hatch part are show in Fig.8a and b. As can be seen, for the wing-skin part, the optimized orientation is 95.6°, where the maximum positional offset of the GND electrodes is 24.3 mm. For hatch part, the optimized orientation is 30.9°, where the maximum positional offset of the GND electrodes is only 2.94 mm. The rectangular strip arrangements of the initial orientation and the optimal orientation are shown in Fig.8 c, d. It can be clearly seen that by regulating the orientation of the strip, the positional offset of the GND electrodes is significantly reduced. The reductions of 84.97% and 94.42% for the wing-skin and hatch parts are respectively achieved.

The multi-zone SRE heating processes of two parts under the initial and the optimized strips orientations are further simulated by FEM method. The two different strip arrangement of the wing-skin part obtained different simulation results. The simulated temperature field of the wing-skin part is shown in Fig. 9a, d. First, the side of the left end is selected as the GND electrodes, and the maximum offset among GND electrodes reaches 161.7 mm. There are three local overheating spots and the temperature on the left side of the part is very low. This is attributed that there is large transverse potential gradient and the current density is non-uniform, as shown in Fig.9b. The maximum average temperature difference reaches 66.4 °C, as shown in Fig.9c. The temperature field after optimizing the

orientations of the strips is shown in Fig. 9d. It can be seen that the maximum average temperature difference is only 2.61°C, as shown in Fig.9f, which reduces by 96.1% after prioritizing the orientation of the strips. In Fig.9e, the positional offset of the GND electrodes of the strip is only 24.3 mm, and the transverse potential gradient can be almost ignored as shown in Fig. 9e. The current density is uniformly distributed, and there is no obvious overheated point. Therefore, the temperature uniformity of the wing-skin part is effectively improved by using the optimized multi-zoning method.

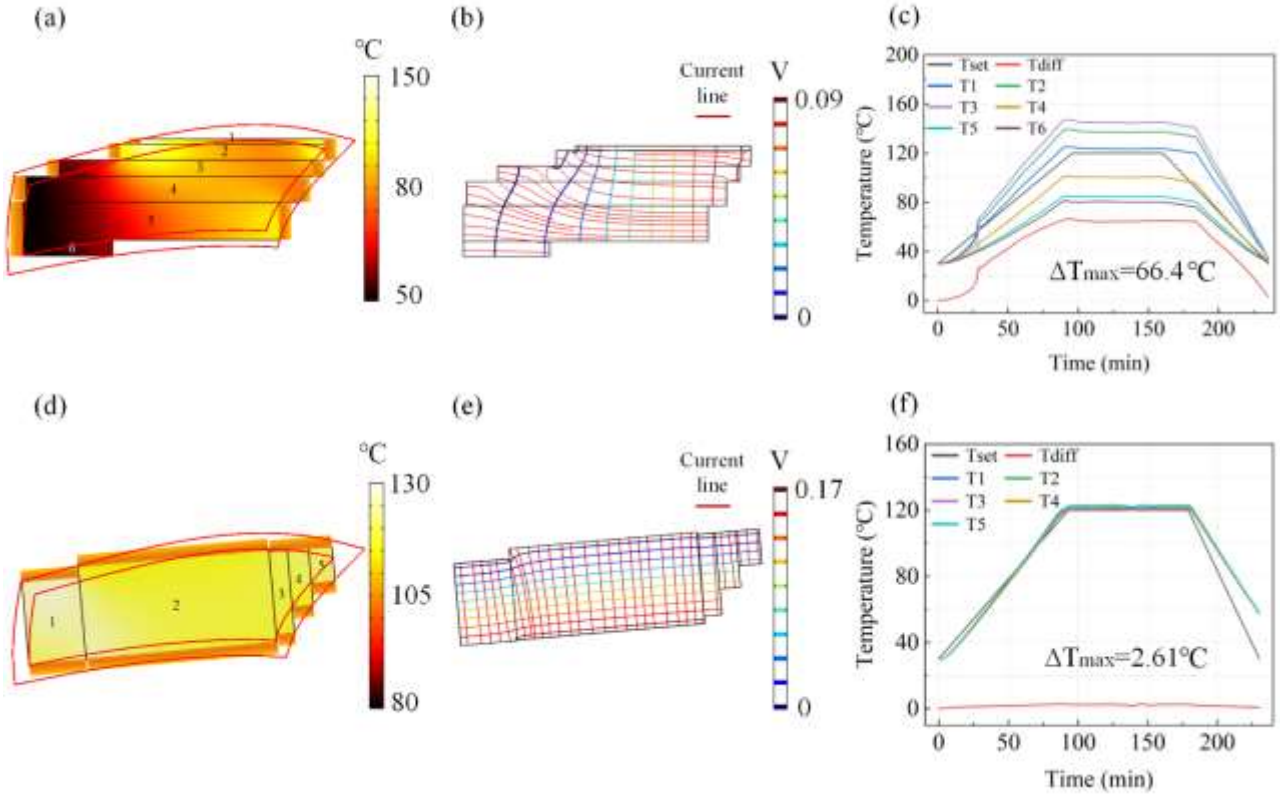

Fig.9 Simulated results of the wing-skin part **a** temperature field of non-optimized strips wing-skin part **b** current line and potential line of non-optimized wing-skin part **c** temperature data of non-optimized strips wing-skin part **d** temperature field of optimized stirps wing-skin part **e** current line and potential line of optimized wing-skin part **f** temperature data of optimized wing-skin part

Fig.10 shows the simulated results of the hatch part. Fig.10a gives the temperature field of the non-optimized SRE heating method where the strip orientation is 0°. The right side of the part is the GND electrodes, and the maximum positional offset of the GND electrodes is 52 mm. The entire left end of the part exhibits overheating, and maximum average temperature difference reaches 34.8 °C, as shown in Fig.10c. In Fig.10b, the current density of the left side is greater than that of the right side, leading to non-uniform distribution of Joule heat. After prioritizing the strip orientation, the temperature uniformity shows a significantly improvement, as shown in Fig.10d. The maximum average temperature difference is only 7.41°C, as shown in Fig.10f, which is reduced by 78.7% compared to that of the non-optimized part. In Fig.10e, the potential gradients and current densities at the VCC and GND electrodes position are uniformly distributed.

The above content demonstrates the effectiveness of the proposed method on two typical shaped CFRP parts. Regarding the robustness of the method in different cases, the proposed method is based on the principle of optimization after traversal calculation of all orientation of strips, and to a certain extent, an optimal orientation could always be found, but the optimization performance for some complex parts may decline.

This chapter presents the optimized multi-zoning method for shaped parts, which can significantly decrease the

positional offset of the GND electrodes by prioritizing the strips orientation, and further notably improve the temperature uniformity because the transverse voltage gradient between strips and the accompanying local overheating is effectively suppressed. Through this method, the maximum in-plane temperature difference of shaped CFRP parts is controlled within 10°C, which meets the actual curing requirements. Next, in order to further verify the effectiveness of the method, the experimental validation are carried out on the wing-skin part.

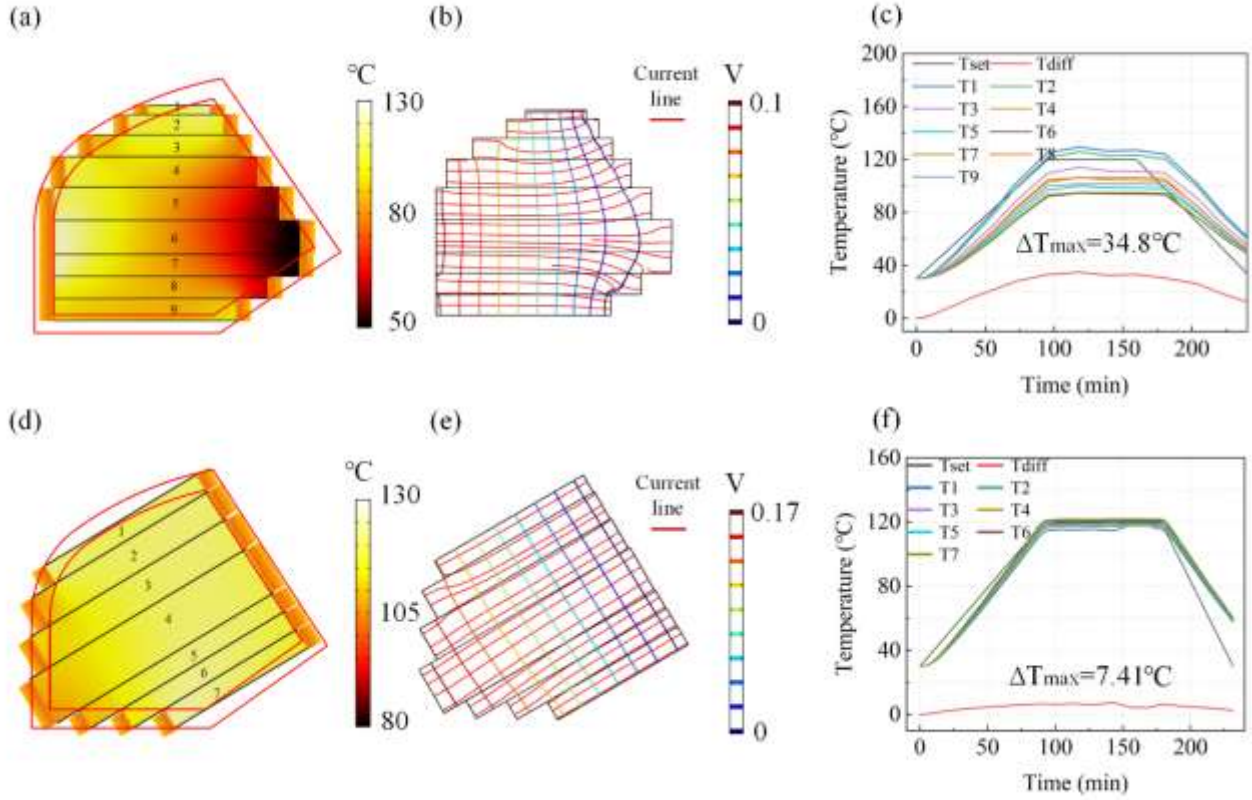

Fig.10 Simulated results of the hatch part **a** temperature field of non-optimized strips hatch part **b** current line and potential line of non-optimized hatch part **c** temperature data of non-optimized strips hatch part **d** temperature field of optimized stirps hatch part **e** current line and potential line of optimized hatch part **f** temperature data of optimized hatch part

4. Experimental validation

This chapter demonstrates the experimental cases of the wing-skin parts cured by the traditional SRE heating method and the multi-zone SRE heating method with the initial and optimized strip orientations. The following sections introduce the experimental arrangement and results respectively.

4.1 Experimental arrangement

Material: The CFRP material system UIN10000/T800 unidirectional prepreg (China Weihai Guangwei composite co., LTD) with a resin content of 30% and a thickness of about 0.1 mm per layer is employed in this study. The lay-up sequence schematic of CFRP laminates with electrodes arrangement is shown in Fig.11. For the wing-skin part, 30 layers of unidirectional UIN10000 prepreg are stacked with a sequence of 0°/90°, and the size of the final cured part is about 600 mm long, 180 mm wide, and 3 mm thick. The red copper electrodes of 0.02 mm thick with a purity of 99.7% is layer-by-layer stacked along the side edge of multiple CFRP strips. As illustrated in Fig.12, the edge of each stack of electrodes is connected to a cable. Each cable with silicone rubber insulation can suffer a maximum current of 50A and a Q235 steel tooling with thick of 8 mm is used. In the SRE curing process, the polyimide film (Meixin insulation materials Co., LTD) is used for insulating between the composites and the metal tooling. The auxiliary material used in the experiment is purchased from supplier Airtech International, Inc., such as

the L500Y vacuum bag, PMMA release film, B150 breather.

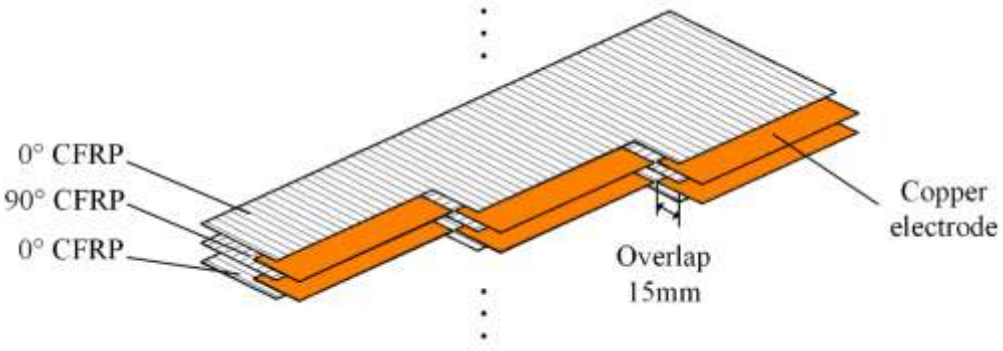

Fig.11 Schematic of CFRP laminates lay-up sequence and electrodes arrangement

Multi-generators-based heating system: Shaped CFRP parts are heated by multiple direct current (DC) generators based heating system, where the output voltage of each generator is independently controlled by a proportional–integral–derivative (PID) controller [29,30]. The maximum power output of each DC generator (SZPAIER co., LTD) is 500 A, and the rated power is 5 kW. Each PID temperature controller (AI516P, Xiamen Yudian Auto Tech Co., Ltd.) receives the corresponding temperature feedback from a specific K-type thermocouple (WRNK-191, Xingke Co., Ltd.) that is contacted with the target strip. The PID controller continuously calculates an error value $e(t)$ as the difference between the desired setpoint (SP) and a measured process variable (PV) and applies a correction based on proportional, integral, and derivative terms (denoted by P, I, and D respectively). The temperature values of all the strips are recorded by a temperature recorder TP700(Shenzhen Top Purui Electronics Co., Ltd.). The SRE heating temperature field under the heating process is observed by the infrared (IR) thermal image camera (Flir A300). In addition, for the case of the traditional SRE heating process with the integral electrodes, 3 distributed thermocouples are simultaneously applied, and their average temperature is calculated in real-time and feed-back to a single PID controller.

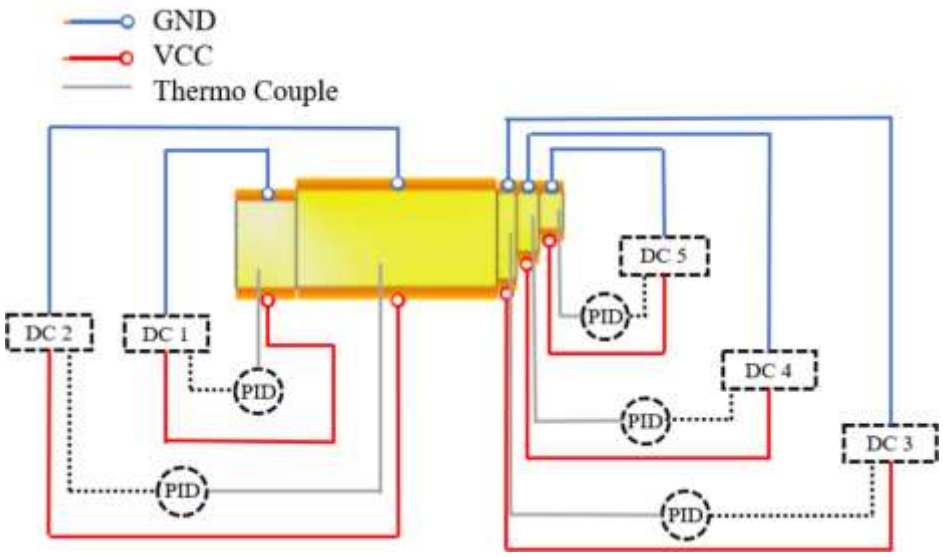

Fig.12 Arrangement schematic of the DC power supply, thermocouples and cables

Vacuum bagging: The whole bagging system from the bottom to the top is consisted of tooling, polyimide, wing-skin part, peel-ply, isolator, breather, and vacuum bag, as shown in Fig.13. By placing a polyimide film with a thickness of 0.05 mm as an insulating layer between the tooling and the wing-shaped part, the electric current passing through the inside of the material is prevented from being conducted into the steel mold. The curing process is

performed under a vacuum bag pressure of 0.095 MPa. Cables are welded by the solder with the copper electrodes. The cables also sealed by the sealing tape between the vacuum bag and the tooling. Three different wing-skin parts including the integral electrodes connected part (traditional), the multi-zone part with the initial strip orientation (non-optimized), and the multi-zone part with optimized strip orientation are produced as shown in Fig.14.

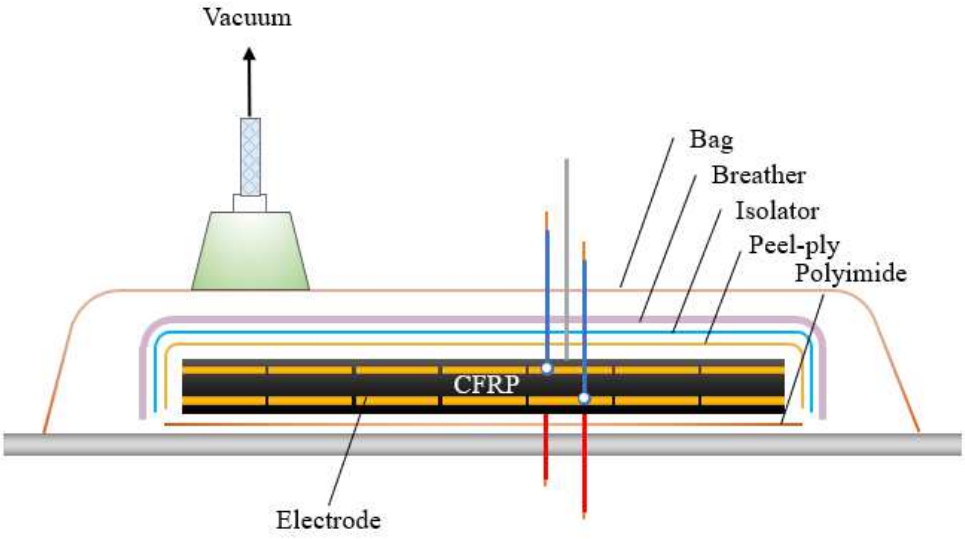

Fig.13 Arrangement schematic of the vacuum bagging process

Fig.14 Bagging arrangement photos of the **a** integral electrodes (traditional SRE method) part, **b** multi-zone part with non-optimized strip orientation, and **c** multi-zone part with optimized strip orientation.

4.2 Result and discussion

The presented multi-zone heating method considers the minimized positional offset of equipotential points in adjacent strips, and can suppress the transverse voltage gradient and the accompanying local overheating. By demonstrating the IR images and the temperature curves, this section demonstrates the effectiveness of the presented method in improving the temperature uniformity of shaped parts in the SRE heating process.

Fig. 15a shows the IR image of the wing-skin part heated by the traditional SRE heating method where the integral electrodes are used at the edge of the part. A hot spot appears at the center area near to the VCC electrode, but the right corner of the part remains in cold. The maximum in-plane temperature difference among the measured points T1-T4 reaches 89.6°C as shown in Fig. 15b. This is attributed to that the current density and the generated Joule heat is unevenly distributed in the part due to the irregular shape of the conductive structure. As a result, as shown in Fig.16a, because the right corner of the part is not heated to the vitrification temperature, the material is still soft, sticky, and not rigid enough.

Fig.15c shows the multi-zone SRE heating temperature field under the initial orientation (0°) of strips where the GND side has a maximum positional offset of 161.7 mm. Obviously, although the power of each strip is independently controlled according to the temperature feedback, a uniform temperature field is not formed in the part as expected. Specifically, the IR image shows the thermal accumulation at the corner of contiguous lines between strips. The maximum in-plane temperature difference measured by the thermocouples T1-T5 is 43.7°C as shown in

Fig.15d. During the curing process, to reduce the temperature difference between the strips, an attempt is made to cool down the early stage of the dwelling process, but the improvement is not noticeable. In addition, the IR image shown in Fig.15c is consistent with the simulated temperature field in Fig.9a. This shows that in the actual SRE heating process, a transverse voltage gradient is also formed between different strips, which leads to the current lines gathering at these areas, causing multiple undesired overheating points. In Fig.16b, the corresponding hot points show a serious thermal degradation of the resin after curing, which is unacceptable to the performance of the material even within the net-shape of the part. It can be seen from the results that the existing MZC method does not consider the offset of the equipotential points of adjacent strips, and it will be difficult to achieve a uniform SRE heating of the shaped part.

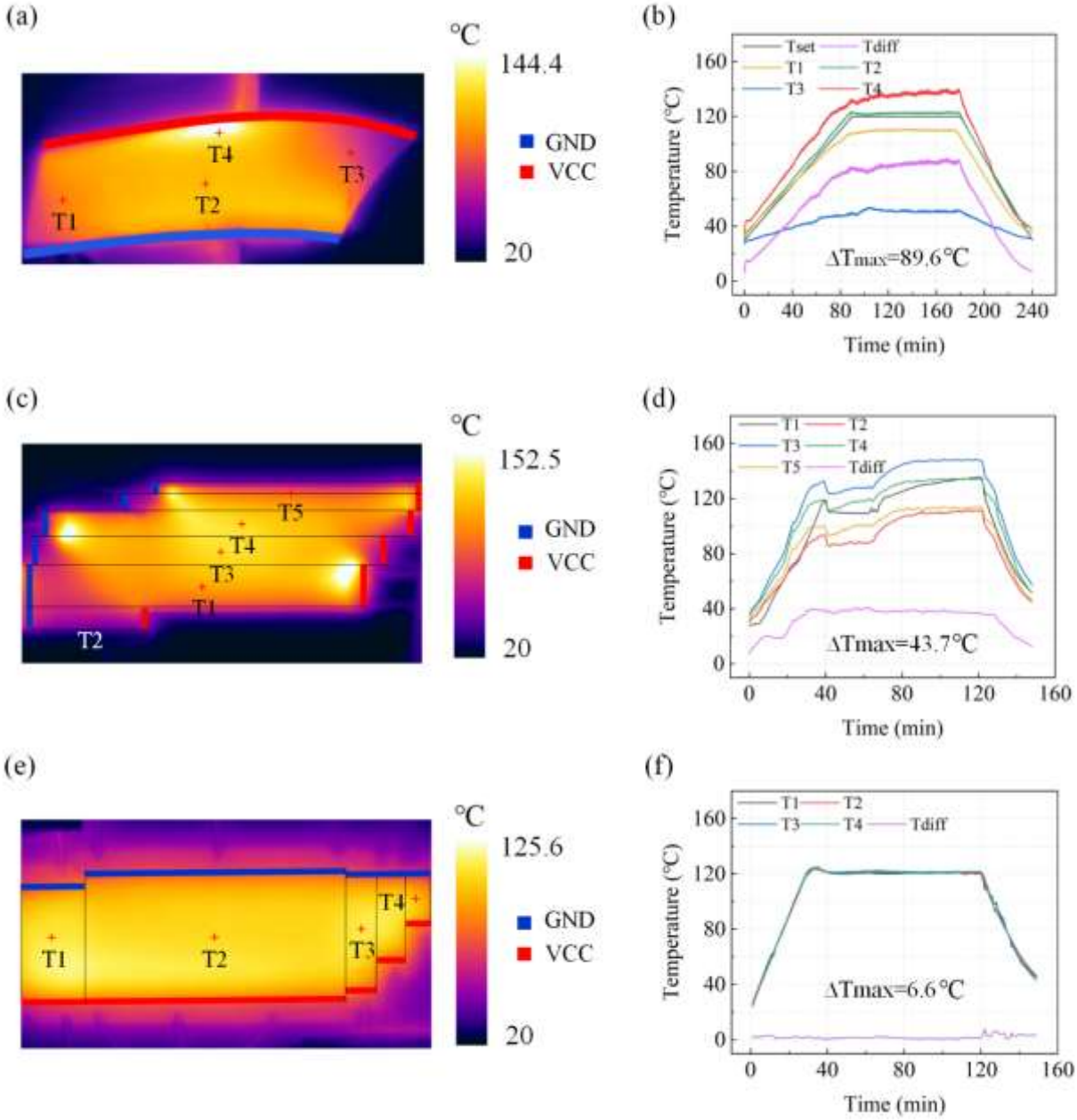

Fig.15 Temperature field result **a, c, e** SRE heating infrared images of integral electrode, non-optimized and optimized orientation of strips CFRP parts **b, d, f** Temperature data of shaped CFRP

Fig.15e illustrates the SRE heating temperature field under the optimal strip orientation (95.6°) where the GND side has a positional offset of only 24.3 mm. It can be seen from the figure that there is no local overheating in the

entire part surface, which is highly consistent with the simulated temperature field in Fig.9d. The maximum in-plane temperature difference measured by the thermocouple T1-T4 is only 6.6°C, which is 84.9% decreased compared to that of the non-optimized method, and meets the curing requirement that the maximum temperature difference is less than 20°C when the average temperature is 120°C during the curing process of CFRP materials. This shows that through the optimized multi-zone SRE heating method proposed in this paper, an optimal strip orientation that has the minimized offset of the GND electrodes can always be found, so that the transverse voltage gradient and the accompanying local overheating can be effectively suppressed. However, it can also be seen from Fig.15e that the temperature at the edge of the part is lower than that at the center area, which is due to the heat absorption of the larger area of the tooling, which can be improved by applying insulation to the tooling and parts. In Fig.16c, the final wing-part obtains a smooth surface where no uncured or thermal degradation area can be found.

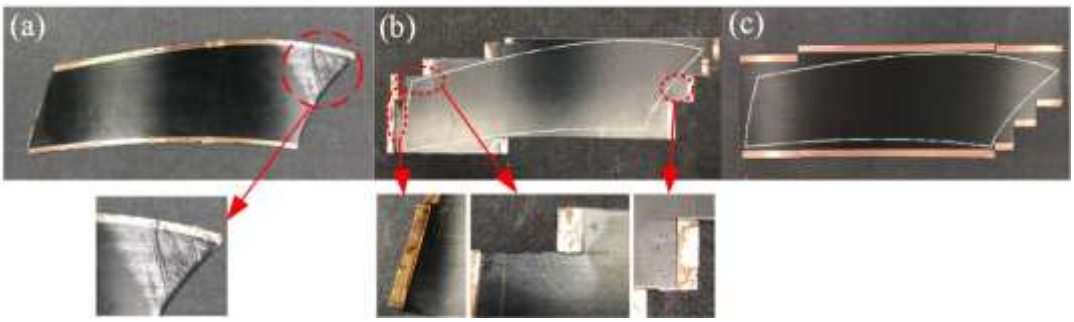

Fig.16 Finished part **a** Integral electrode SRE heating part **b, c** CFRP parts with non-optimized and optimized orientation of strips

From the above result, it is concluded that by using the presented method, the optimal strip orientation considering the minimized positional offset of the electrodes can be found, which realizes a notable improvement of the temperature uniformity for the shaped part during the SRE heating process. The maximum in-plane temperature difference of the optimized wing-shaped part is only 6.6°C, which is 84.9% lower compared to the SRE heating method with that of the non-optimized multi-zone SRE heating method.

5. Conclusion

In this paper, an optimized multi-zone SRE heating method is proposed, in which the uniform SRE heating and curing process of the shaped CFRP part is firstly achieved. The MZC method based multi-zone SRE heating have been successfully applied in the metal blank heating processes. However, the existing methods do not consider the transverse voltage gradient caused by the positional offset of the electrodes in adjacent strips, which results in local overheating and the unacceptable large temperature gradient. In the proposed method, by optimizing the orientation of the rectangular zones, the local overheating caused by the voltage gradient and current diffusion between zones is notably suppressed. From the result of the electro-thermal numerical analysis, the positional offset of the GND electrodes has a significant impact on the final temperature uniformity, and the offset of VCC electrodes has less influence on the temperature field under the thermal isolation condition. Based on this influential law, an automated zoning algorithm and the prioritizing method of the zone orientation are established. Based the numerically and experimentally validations on the typical shaped CFRP parts, the proposed method realizes a significant reduction of more than 80% of in-plane temperature difference compared with the existing SRE heating method.

Furthermore, the influence of uneven heat in-plane dissipation on the temperature field should be further considered to improve the temperature uniformity of SRE heating process. The proposed method firstly realizes the SRE heating of shaped CFRP part with a uniform temperature distribution, which provides a potential solution for the high-quality and efficient curing of practical CFRP parts.

Acknowledgements The authors would like to acknowledge the team members, for their continuous support.

Funding This work was supported by Major project of National Natural Science Foundation of China (Grant no. 52090052), National Natural Science Foundation of China (Grant no. 51775261) and Postgraduate Research & Practice Innovation Program of Government of Jiangsu Province (KYCX18_0319), the authors sincerely appreciate the continuous support provided by our industrial collaborators.

Declarations

Data availability Not applicable for that section.

Code availability Not applicable for that section.

Ethics approval Not applicable for that section.

Consent to participate Not applicable for that section.

Consent for publication Not applicable for that section.

Conflict of interest Not applicable for that section.

Reference

1. Hamerton I, Mooring L (2012) The use of thermosets in aerospace applications. In: Thermosets. Elsevier, pp 189–227
2. Soutis C (2005) Fibre reinforced composites in aircraft construction. Progress in Aerospace Sciences 41:143–151. https://doi.org/10.1016/j.paerosci.2005.02.004
3. Friedrich K, Almajid AA (2013) Manufacturing Aspects of Advanced Polymer Composites for Automotive Applications. Appl Compos Mater 20:107–128. https://doi.org/10.1007/s10443-012-9258-7
4. Mishnaevsky L, Branner K, Petersen H, Beauson J, McGugan M, Sørensen B (2017) Materials for Wind Turbine Blades: An Overview. Materials 10:1285. https://doi.org/10.3390/ma10111285
5. Tang DZ (2013) The Application of Carbon Fiber Materials in Sports Equipment. AMM 443:613–616. https://doi.org/10.4028/www.scientific.net/AMM.443.613
6. Maria M (2013) The faculty of operation and economics of transport the air transport department univerzitna, Advanced composite materials of the future in aerospace industry. INCAS BULLETIN 5:139–150. https://doi.org/10.13111/2066-8201.2013.5.3.14
7. Mujahid Y, Sallih N, Abdullah MZ, Mustapha M (2021) Effects of processing parameters for vacuum-bag-only method on void content and mechanical properties of laminated composites. Polym Compos 42:567–582. https://doi.org/10.1002/pc.25848
8. Liu W, Li L, Zhang S, Yang F, Wang RG (2017) Mechanical properties of carbon nanotube/carbon fiber reinforced thermoplastic polymer composite. Polym Compos 38:2001–2008. https://doi.org/10.1002/pc.23771
9. Abliz D, Duan Y, Steuernagel L, et al (2013) Curing Methods for Advanced Polymer Composites - A Review. Polym Compos 21:9 https://doi.org/10.1177/096739111302100602
10. Zhou J, Li Y, Li N, Y, Liu ST, Cheng LB, Sui SC, Gao J (2018) A multi-pattern compensation method to ensure even temperature in composite materials during microwave curing process. Compos Part A Appl Sci Manuf 107:10–20. https://doi.org/10.1016/j.compositesa.2017.12.017
11. Xu XH, Wang XQ, Wei R, Du SY (2016) Effect of microwave curing process on the flexural strength and interlaminar shear strength of carbon fiber/bismaleimide composites. Compos Sci Technol 123:10–16. https://doi.org/10.1016/j.compscitech.2015.11.030
12. Bayerl T, Duhovic M, Mitschang P, Bhattacharyya D (2014) The heating of polymer composites by electromagnetic induction– a review. c 57:27–40. https://doi.org/ 10.1016/j.compositesa.2013.10.024
13. Riccio A, Russo A, Raimondo A, Cirillo P, Caraviello A (2018) A numerical/experimental study on the induction heating of adhesives for composite materials bonding. Mater Today Commun 15:203–213. https://doi.org/10.1016/j.mtcomm.2018.03.008

14. Liu S, Li Y, Xiao S, Wu T (2019) Self-resistive electrical heating for rapid repairing of carbon fiber reinforced composite parts. J Reinf Plast Comp 38:495–505. https://doi.org/10.1177/0731684419832793
15. Lackmann J, Konrad S, Lambers H G, Huschen U (2015) Heating device for conductive heating a sheet metal blank. US 2015/0282253 A1
16. Matsumoto S, Yamanishi K (2011) Energization heating method and energization heating device. US 8,866,046 B2
17. Machrowicz T (2007) Method and apparatus for the uniform resistance heating of articles. US 07714253 B2.
18. Behrens BA, Hübner S (2014) Konductive Erwarmung von Formplatinen für das Pressharten, Tech. Rep. 400. Institut für Umformtechnik und Umformmaschinender Leibniz Universit¨at Hannover
19. Demazel N, Laurent H, Carin M, Co¨er J, Le Masson P, Favero J, Canivenc R, Graveleau S (2016) Simulations of joule effect heating in a bulge test. AIP conference proceedings, vol. 1769 2016: 060014. https://doi.org/10.1063/1.4963450
20. Hübner S (2015) Method for conductively heating sheet metal, electrode, and heating device therefore. EP 3259377 A1
21. Demazel N, Laurent H, Carin M, Le Masson P, Salmon-Legagneur H (2021) A direct resistance heating method for shaped blank. J Manuf Process 62:772–783. https://doi.org/10.1016/j.jmapro.2020.12.056
22. Zhang B, Li Y, Liu S, et al (2021) Layered self-resistance electric heating to cure thick carbon fiber reinforced epoxy laminates. Polym Compos 42:2469–2483. https://doi.org/10.1002/pc.25992
23. Raoelison R, Fuentes A, Pouvreau C, Rogeon P, Carr´e P, Dechalotte F (2014) Modeling and numerical simulation of the resistance spot welding of zinc coated steel sheets using rounded tip electrode: analysis of required conditions. Appl Math Modell;38(9–10):2505–21. https://doi.org/10.1016/j.apm.2013.10.060
24. Zhao K, Wietbrock B, Hirt G (2011) Numerical and experimental analysis of electric conductive heating for micro warm coining of stainless steel. German Academic Society for Production Engineering; p.11. https://doi.org/10.1007/s11740-011-0345-7
25. Martins JMP, Alves JL, Neto DM (2016) Numerical analysis of different heating systems for warm sheet metal forming. Int J Adv Manuf Technol 83:897–909. https://doi.org/10.1007/s00170-015-7618-9
26. Athanasopoulos N, Kostopoulos V (2012) Resistive heating of multidirectional and unidirectional dry carbon fibre preforms. Compos Sci Technol 72:1273–1282. https://doi.org/10.1016/j.compscitech.2012.04.018
27. Liu S, Li Y, Shen Y, Lu Y (2019) Mechanical performance of carbon fiber/epoxy composites cured by self-resistance electric heating method. Int J Adv Manuf Technol 103:3479–3493. https://doi.org/10.1007/s00170-019-03707-0
28. Hassan MH, Othman AR, Kamaruddin S (2017) A review on the manufacturing defects of complex-shaped la minate in aircraft composite structures. Int J Adv Manuf Technol 91:4081–4094. https://doi.org/10.1007/s0017 0-017-0096-5
29. Taysom BS , Sorensen CD , Hedengren JD (2017) A comparison of model predictive control and PID temperature control in friction stir welding. J Manuf Process:232-241. https://doi.org/10.1016/j.jmapro.2017.07.015
30. Cominos P, Munro N (2002) PID controllers: recent tuning methods and design to specification. IEE Proceedings-Control Theory and Applications, 149(1): 46-53. https://doi.org/10.1049/ip-cta:20020103

Figure captions

Fig.1 Schematic of the 3D structure used for investigating the effect of temperature field uniformity

Fig.2 Schematic of positional offset of GND electrodes influence. **a** influence on the electric potential field, **b** influence on the current line, **c** influence on the temperature field

Fig.3 Temperature difference as a function of relative position of the ground electrodes

Fig.4 Schematic of positional offset of VCC electrodes influence. **a** influence on the electric potential field, **b** influence on the current line, **c** influence on the temperature field

Fig.5 Schematic of ASD algorithm

Fig.6 Schematic of prioritizing the optimal orientation according to the minimum positional offset of GND electrodes

Fig. 7 Two typical CFRP part **a** Wing-skin part **b** Hatch part

Fig.8 Prioritizing results of two typical parts **a,b** maximum positional offset of the GND electrodes for the wing-skin and the hatch part, **c,d** the rectangular strip arrangements of the initial and optimal orientation for the wing-skin and the hatch part

Fig.9 Simulated results of the wing-skin part **a** temperature field of non-optimized strips wing-skin part **b** current line and potential line of non-optimized wing-skin part **c** temperature data of non-optimized strips wing-skin part **d** temperature field of optimized stirps wing-skin part **e** current line and potential line of optimized wing-skin part **f** temperature data of optimized wing-skin part

Fig.10 Simulated results of the hatch part **a** temperature field of non-optimized strips hatch part **b** current line and potential line of non-optimized hatch part **c** temperature data of non-optimized strips hatch part **d** temperature field of optimized stirps hatch part **e** current line and potential line of optimized hatch part **f** temperature data of optimized hatch part

Fig.11 Schematic of CFRP laminates lay-up sequence and electrodes arrangement

Fig.12 Arrangement schematic of the DC power supply, thermocouples and cables

Fig.13 Arrangement schematic of the vacuum bagging process

Fig.14 Bagging arrangement photos of the **a** integral electrodes (traditional SRE method) part, **b** multi-zone part with non-optimized strip orientation, and **c** multi-zone part with optimized strip orientation.

Fig.15 Temperature field result **a, c, e** SRE heating infrared images of integral electrode, non-optimized and optimized orientation of strips CFRP parts **b, d, f** Temperature data of shaped CFRP

Fig.16 Finished part **a** Integral electrode SRE heating part **b, c** CFRP parts with non-optimized and optimized orientation of strips